

# K<sup>+</sup> versus Na<sup>+</sup> Ions in a K Channel Selectivity Filter: A Simulation Study

Indira H. Shrivastava, D. Peter Tieleman, Philip C. Biggin, and Mark S. P. Sansom

Laboratory of Molecular Biophysics, Department of Biochemistry, University of Oxford, Oxford OX1 3QU, United Kingdom

**ABSTRACT** Molecular dynamics simulations of a bacterial potassium channel (KcsA) embedded in a phospholipid bilayer reveal significant differences in interactions of the selectivity filter with K<sup>+</sup> compared with Na<sup>+</sup> ions. K<sup>+</sup> ions and water molecules within the filter undergo concerted single-file motion in which they translocate between adjacent sites within the filter on a nanosecond timescale. In contrast, Na<sup>+</sup> ions remain bound to sites within the filter and do not exhibit translocation on a nanosecond timescale. Furthermore, entry of a K<sup>+</sup> ion into the filter from the extracellular mouth is observed, whereas this does not occur for a Na<sup>+</sup> ion. Whereas K<sup>+</sup> ions prefer to sit within a cage of eight oxygen atoms of the filter, Na<sup>+</sup> ions prefer to interact with a ring of four oxygen atoms plus two water molecules. These differences in interactions in the selectivity filter may contribute to the selectivity of KcsA for K<sup>+</sup> ions (in addition to the differences in dehydration energy between K<sup>+</sup> and Na<sup>+</sup>) and the block of KcsA by internal Na<sup>+</sup> ions. In our simulations the selectivity filter exhibits significant flexibility in response to changes in ion/protein interactions, with a somewhat greater distortion induced by Na<sup>+</sup> than by K<sup>+</sup> ions.

## INTRODUCTION

Ion channels are involved in many aspects of membrane physiology and are found in organisms ranging in complexity from viruses (Pinto et al., 1997; Plugge et al., 2000) to mammals. They play an essential role in generating and regulating the electrical activity of cells in the nervous system (Hille, 1992). Malfunctions of ion channels are frequently associated with neurological diseases (channelopathies) (Ashcroft, 2000). It is therefore essential to be able to explain ion channel function at a molecular level. This has become possible as a result of recent progress in determination of x-ray structures for ion channels, such as that of KcsA, a bacterial homolog of mammalian K channels (Doyle et al., 1998), and that of MscL, a bacterial mechanosensitive channel (Chang et al., 1998).

A key property of all ion channels is their selective permeability; i.e., only certain species of ion may pass through a channel. Potassium channels are able to select between K<sup>+</sup> ions in favor of Na<sup>+</sup> ions, despite only a small difference in their ionic (i.e., Pauling) radii (0.133 nm vs. 0.095 nm, respectively). Theories of the physical origins of ion selectivity have a long and distinguished history (Hille, 1992). Site-directed mutation studies (Miller, 1991; Lü and Miller, 1995) have shown that a TVGYG signature sequence is associated with the ion selectivity of K channels. The three-dimensional structure of KcsA reveals this se-

quence motif to form a narrow selectivity filter. It has been suggested that this achieves ion selectivity by having the correct geometry for effective solvation of a K<sup>+</sup> ion by eight peptide oxygen (O) atoms, whereas the pore is too wide to allow proper solvation of the smaller Na<sup>+</sup> ion. This requires interactions of the filter with the rest of the protein to retain a rigid conformation.

In common with other potassium channels, KcsA is more permeable to K<sup>+</sup> ions than to Na<sup>+</sup> ions, although there is some debate as to the exact value of  $P_{Na}/P_K$  (Heginbotham et al., 1999; LeMasurier et al., 2000; Schrepf et al., 1995; Meuser et al., 1999; LeMasurier et al., 2001). Furthermore, intracellular Na<sup>+</sup> ions can block KcsA (Heginbotham et al., 1999) and other K channels, and at sufficiently high voltages intracellular Na<sup>+</sup> ions can permeate KcsA via a “punch-through” mechanism (Nimigeon and Miller, 2002). There is good evidence that KcsA is representative of mammalian K channels, especially Kv channels (MacKinnon et al., 1998; LeMasurier et al., 2001), and thus may be expected to share their selectivity properties. As summarized by Hille (1992), K channels are highly selective to K<sup>+</sup> ions over Na<sup>+</sup> ions. However, it is possible for Na<sup>+</sup> ions, under certain circumstances, to pass through K channels. For example, French and Wells (1977) demonstrated outward Na<sup>+</sup> permeability of Kv channels at high voltages. More recently, studies of Kv2.1 have shown a Na<sup>+</sup> conductance in the absence of K<sup>+</sup> ions (Korn and Ikeda, 1995; Kiss et al., 1998). Na<sup>+</sup> permeability of Kv channels in the absence of K<sup>+</sup> has been interpreted in terms of changes in conformation of the selectivity filter (Immke et al., 1999; Loboda et al., 2001). Furthermore, relatively conservative mutations in the filter region can enhance the Na<sup>+</sup> selectivity of K channels. In a careful study of the effects of selectivity mutations in the TVGYG filter sequence of *Shaker* Kv channels on their ion selectivity (Heginbotham et al., 1994) estimated  $P_{Na}/P_K < 0.02$  for wild-type channels, this value rising to  $< 0.2$  for a mutation in which the key Y residue was replaced by a V. In Kir6.2 channels (Proks et al., 2001) the

Submitted July 16, 2001, and accepted for publication April 17, 2002.

I. H. Shrivastava's current address: LEC, CCR, NIC, MSC 5677, Bethesda, MD 20892.

D. P. Tieleman's current address: Department of Biological Sciences, University of Calgary, 2500 University Dr. NW, Calgary, Alberta T2N 1N4, Canada.

Address reprint requests to Dr. Mark S. P. Sansom, Laboratory of Molecular Biophysics, The Rex Richards Building, Department of Biochemistry, University of Oxford, South Parks Road, Oxford OX1 3QU, UK. Tel.: 44-1865-275371; Fax: 44-1865-275182; E-mail: mark@biop.ox.ac.uk.

© 2002 by the Biophysical Society

0006-3495/02/08/633/13 \$2.00

Y is replaced by a F and  $P_{\text{Na}}/P_{\text{K}} = 0.27$ . Thus, the filter region of K channels can under certain circumstances accommodate  $\text{Na}^+$  ions, albeit less favorably than it does  $\text{K}^+$  ions.

It is possible to use atomistic simulations (Roux and Karplus, 1994; Woolf and Roux, 1994; Tieleman and Berendsen, 1998; Tieleman et al., 1999; Bernèche and Roux, 2000, 2001; Forrest and Sansom, 2000; Sansom et al., 2000; Chung et al., 2002) to explore the relationship between the structure of a channel and its functional properties (as reviewed by Roux et al., 2000; Tieleman et al., 2001). In particular, simulations of KcsA have been used to explore the physical basis of ion selectivity (Guidoni et al., 1999; Allen et al., 1999, 2000; Åqvist and Luzhkov, 2000; Biggin et al., 2001). Although there are differences in interpretation of the results from these various studies, they agree with one another in highlighting differences between the interactions of  $\text{K}^+$  ions and of  $\text{Na}^+$  ions with the selectivity filter of the channel protein.

In the present paper we compare simulations of the interactions of KcsA with  $\text{K}^+$  ions versus  $\text{Na}^+$  ions in the selectivity filter. The duration of these simulations ( $\sim 2$  ns) corresponds to the mean passage time of an ion for a channel of conductance of  $\sim 800$  pS at 100 mV membrane potential. As the measured conductance of KcsA is  $\sim 80$  pS (Heginbotham et al., 1999), this implies that our simulations are an order of magnitude shorter than the mean time it takes for a single ion to fully traverse the channel. However, based on previous simulation studies (Shrivastava and Sansom, 2000; Bernèche and Roux, 2000) we can expect to see short time- and length-scale motions of ions within the selectivity filter. By comparing the behavior of  $\text{K}^+$  and of  $\text{Na}^+$  ions in the filter we suggest a model for the experimentally observed selectivity that represents a refinement of earlier models (see, e.g., Armstrong, 1998) that focused upon a rigid geometry for the selectivity filter, as opposed to the flexibility that is observed in simulations.

## METHODS

### System setup

All simulations were based on the same protein coordinate set, corresponding to a minor modification of PDB file 1bl8 (Doyle et al., 1998). KcsA side-chain coordinates missing from the PDB file were added by building in stereochemically preferred conformers. In particular, although not present in the x-ray structure, an inter-subunit salt bridge (D80 to R89) was formed during the early stages of the simulations. Note that residues 1–22 and 120–160 are not included in this KcsA model, which therefore represents the core channel-forming domain of the protein. Preliminary simulations (Capener and Sansom, unpublished results) of a model of the intact KcsA protein suggest that the presence of the missing N- and C-terminal regions does not alter events at the selectivity filter. As described in more detail in Shrivastava and Sansom (2000) the KcsA molecule was embedded in a pre-equilibrated palmitoylcholine (POPC) lipid bilayer, using procedures similar to those used in previous membrane protein simulations (Tieleman and Berendsen, 1998; Tieleman et al., 1999). The final bilayer contained 243 POPC molecules, of which 116

**TABLE 1** Summary of simulations

Simulation	Initial occupancy of sites						Parameter
	S0	S1	S2	S3	S4	Cavity	
KA13C		K	W	K		K	A
KA02C	K		K	W		K	A
KB13C		K	W	K		K	B
KA13Cp*		K	W	K		K	A
KA024p*	K	W	K		K		A
NaA13C		Na	W	Na		Na	A
NaA02C	Na		Na	W	Na		A
NaA24C			Na	W	Na	Na	A
NaB13C		Na	W	Na		Na	B
NaA13Cp*		Na	W	Na		Na	A
NaA013p*	Na	Na	W	Na			A

All simulations were of at least 2 ns duration. In KA02C, the starting configuration corresponds to the end of KA13C, except that the third  $\text{K}^+$  ion is repositioned to the extracellular mouth, S0. In NaA13C, the ions and the water at S2 were restrained during the 100-ps equilibration of the system. In NaA02C, the starting configuration corresponds to the end of NaA24C, except that the third  $\text{Na}^+$  ion is repositioned to the extracellular mouth, S0. Simulations are nan [ion][parameter set][initial configuration]; i.e. KA13C has  $\text{K}^+$  ions using parameter set A at sites S1, S3, and Cavity). \*The four simulations named following 'p' had the ionization states of side chains adjusted such that a proton was shared between each Glu71-Asp80 side chain pair (see text for details).

were in the extracellular leaflet and 127 in the intracellular leaflet. The entire system was solvated with 9821 SPC (Berendsen et al., 1981) water molecules. All ionizable side chains were in their default ionization states (other than in KA13Cp, KA024p, NaA13Cp, and NaA013p (see Table 1) in which the ionization states of the Glu71 and Asp80 side chains were adjusted such that a proton was shared between each Glu71-Asp80, in accordance with  $\text{pK}_\text{A}$  calculations (Ranatunga et al., 2001)) and sufficient  $\text{Cl}^-$  counterions were added to give a net charge of zero. The counterions were placed at low potential energy positions.

### Simulation protocol

The simulation protocol was similar to that used previously (Tieleman et al., 1999; Randa et al., 1999; Shrivastava and Sansom, 2000; Capener et al., 2000), using the molecular dynamics (MD) simulation package GROMACS, v1.6 (<http://www.gromacs.org>). Lipid parameters were based on those of Berger et al. (1997) and Marrink et al. (1998) and the protein parameters on GROMOS87. A twin-range cutoff for longer-range interactions was used: 1.0 nm for van der Waals and 1.7 nm for electrostatic interactions. Test simulations using particle-mesh Ewald (Darden et al., 1993) suggest that the treatment of long-range electrostatic interactions does not unduly influence events at the selectivity filter (Shrivastava and Sansom, unpublished results; Capener and Sansom, 2002). The time step was 2 fs, the neighbor list was updated every 10 steps, and the LINCS algorithm (Hess et al., 1997) was used to constrain bond lengths, under NPT conditions. A constant pressure of 1 bar in all three directions was used with a coupling constant of  $\tau_p = 1.0$  ps. Water, lipid, and protein were coupled separately to a temperature bath at 300 K, with a coupling constant of  $\tau_T = 0.1$  ps (Berendsen et al., 1984). Simulations were performed on an 80-node SGI Origin 2000. About 10 days of CPU time on eight processors were needed for 1 ns of simulation time.

### Ion parameters

Two sets of ion parameters were used (see Appendix for a comparison). In most of the simulations the  $\text{K}^+$  and  $\text{Na}^+$  parameters were as in Straatsma

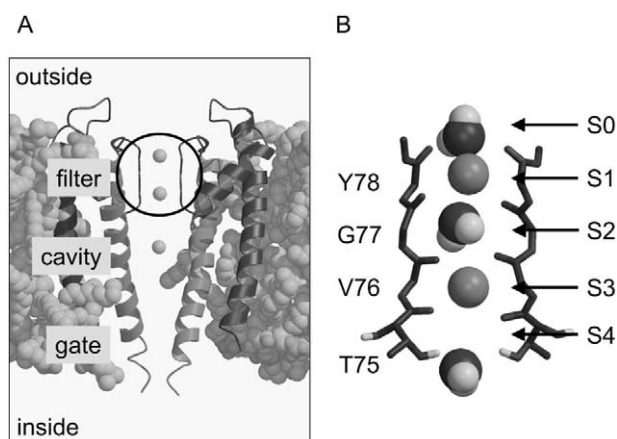


FIGURE 1 Overview of the simulation system (*A*), including a definition of the four sites (S1 to S4) in the selectivity filter (*B*). (*A*) The KcsA channel (shown using two polypeptide chains out of the four) is embedded in a lipid bilayer. The structure of KcsA can be thought of as made up of a selectivity filter (formed by the TVGYG-motifs of the P-loop, a central cavity, and an intracellular gate where the cavity-lining M2 helices pack closely together so as to occlude the central pore). (*B*) The water molecules and  $K^+$  ions in the filter are in the configuration: W(S0)-K1(S1)-W(S2)-K2(S3)-e(S4)-W(C), where S0 is the extracellular mouth, C is the cavity, and e indicates that a site is empty. This corresponds to the initial configuration of simulation KA13C.

and Berendsen (1988). These parameters will be referred to as parameter set A. In two simulations we also employed parameters derived from those in Åqvist (1990), which will be referred to as parameter set B.

## Analysis

Analysis of simulations was performed using GROMACS. Pore radius profiles were calculated using HOLE (Smart et al., 1993). Structure diagrams were drawn using Molscript (Kraulis, 1991) and Raster3D (Merritt and Bacon, 1997).

## RESULTS

### Sites and simulations

In discussing the initial configurations of the system (see Table 1), and the trajectories of the simulations, it is useful to define sites within the selectivity filter (Fig. 1). Sites S1 to S4 form the selectivity filter region. Each site is defined as the center of two rings each containing four O atoms: site S1 is formed by the carbonyl oxygens of residues Y78 and G77; S2 by the carbonyl oxygens of G77 and V76; and S3 by the carbonyl oxygens of V76 and T75. Site S4, which is next to the central water-filled cavity, is formed by one ring of carbonyl oxygens (those of T75) and by a ring of hydroxyl oxygens from the four T75 side chains. One might also add a more poorly defined site (site S0) at the external mouth of the pore, formed by the carbonyl oxygens of residues G79 and Y78.

Simulations have been run with either  $K^+$  ions or  $Na^+$  ions in the filter. Note that the first nanosecond of KA13C

has already been described (Shrivastava and Sansom, 2000). In simulations KA13C and NaA24C two ions ( $K1$  and  $K2$  or  $Na1$  and  $Na2$ , respectively) were initially positioned at two of the sites that are occupied in the x-ray structure, namely S1 and S3, with a water molecule in between. However, during equilibration of NaA24C the  $Na1$  ion moved to S2 and the  $Na2$  ion moved close to S4 (see below). In each case a third ion was positioned in the center of the cavity (Roux and MacKinnon, 1999). Simulation KA02C started with ions  $K1$  and  $K2$  at the locations they had adopted at the end of 1 ns of simulation KA13C (i.e., at sites S3 and just inside the cavity, respectively) with the third ion at the extracellular mouth of the channel, close to S0. NaA02C was a continuation of NaA24C, but with the third ion (which had exited from the channel) displaced to just above the extracellular mouth of the channel, again close to S0. In NaA13C the two ions in the filter and the intervening water molecule were fully restrained during the 100-ps equilibration period. These restraints were removed at the start of the production run. All of the aforementioned simulations used parameter set A for the ions. Simulations KB13C and NaB13C used parameter set B. The initial positions of the ions in KB13C and NaB13C were the same as in KA13C and NaA13C, respectively.

### Ion trajectories in the filter

An immediate impression of the difference in behavior between  $K^+$  and  $Na^+$  ions in the selectivity filter can be obtained by examining the trajectories of the ions projected onto the central pore ( $z$ ) axis (Fig. 2). Note that the center of the filter (here defined as the ring of four V76 carbonyl O atoms) is set to  $z = 0$ , with S1 at  $z \sim +0.5$  nm and S4 at  $z \sim -0.5$  nm.

### KA13C versus NaA13C

Let us first compare KA13C and NaA13C (Fig. 2, *A* and *C*). In both of these simulations the ions are positioned close to the positions of ions in the x-ray structure. It is evident that in KA13C the  $K1$  and  $K2$  ions move through the filter, translocating from site to site on a timescale of  $\sim 0.5$  ns, whereas in NaA13C there is no evidence of concerted translocation of  $Na^+$  ions beyond an initial relaxation (in  $<100$  ps) even when the simulation was extended to 2.8 ns. Note that in KA13C in addition to the concerted translocation of  $K^+$  ions and water along the filter, there is an exchange of a  $K^+$  ion ( $K2$ ) with a water at site S4 (just above the cavity). Thus site S4 is occupied by  $K2$  at  $\sim 900$  ps, when it is exchanged for a water molecule from the cavity (this coincides with the time at which  $K3$  leaves the cavity through the intracellular mouth (see Shrivastava and Sansom, 2000). Thus a K-W-K single file in the filter is replaced by a K-W-W single file. It is noteworthy that all four sites are nearly always occupied, either by a water

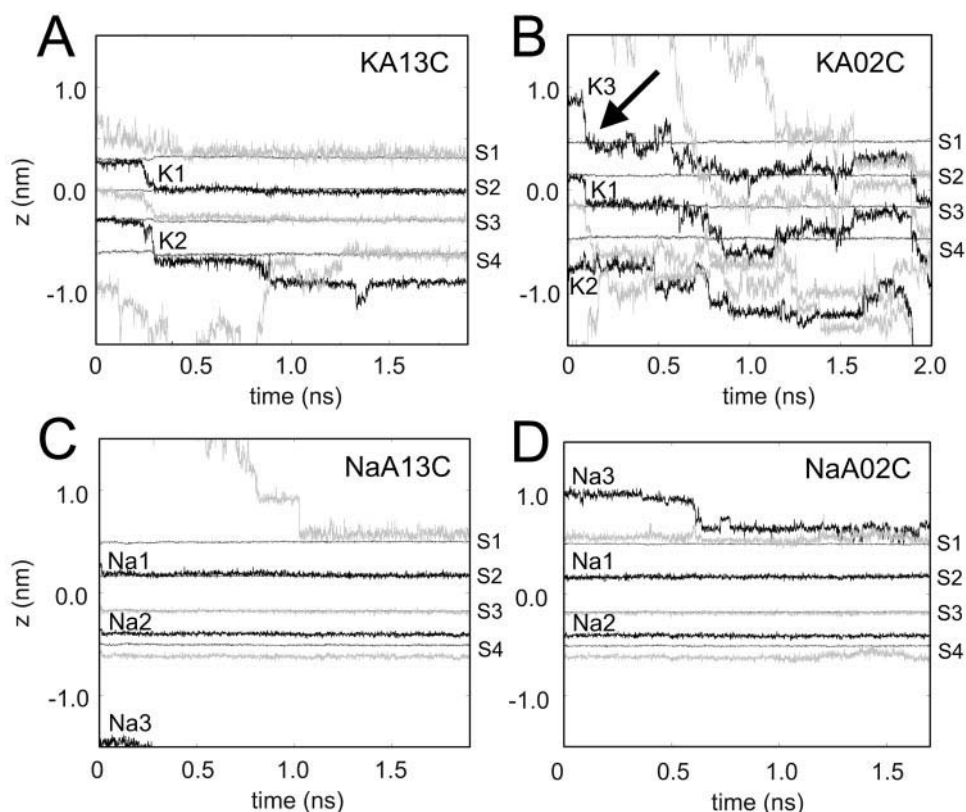


FIGURE 2 Trajectories (along the pore axis) of  $K^+$  or  $Na^+$  ions (thick black lines) and water molecules (gray lines) for simulations: (A) KA13C; (B) NaA13C; (C) KA02C; (D) NaA02C. Note that, for clarity, not all water molecules within the filter are shown. The locations on  $z$  (pore axis) of the four sites (S1 to S4) defined by the geometric center of the 8 oxygen atoms are indicated by the thin black lines. At each point in time, the origin of the coordinate system is defined as the center of gravity of the 16 oxygen atoms that line the selectivity filter. The black arrow in B indicates the time at which a  $K^+$  ion enters the selectivity filter from the extracellular mouth (S0) of the channel.

molecule or an ion, throughout the period of the simulation; i.e., no long-lasting gaps are seen in the single file.

#### KA02C versus NaA02C

Simulations KA02C and NaA02C (Fig. 2, B and D) were set up to study entry of ions into the selectivity filter from the extracellular mouth, as has been studied by Guidoni et al. (1999). The starting structure for KA02C was the 1-ns structure from the simulation KA13C, when K3 had exited through the intracellular mouth of the pore. K3 was repositioned at the extracellular mouth of the selectivity filter, at a distance of 0.75 nm from S1, i.e., close to S0. At the start of KA02C site S1 was occupied by a water molecule. The  $K^+$  ion at S0 (K3) was initially solvated by six water molecules. On reaching S1 it becomes desolvated, and the water molecule at S1 (not shown in Fig. 2 B) moves to S2. At the same time there is a concerted motion of K2 from S3 to S4 and of a water molecule from S2 to S3, resulting in K3 at S1, water at S2, K1 at S3, and a water at S4. During the remainder of this simulation, several further concerted motions are seen. Note that at  $\sim 1500$  ps, K1 moves from S4 to S3, a water moves from S3 to S2, and K3 moves from S2 to

S1. Thus the K-W-K single file is able to undergo concerted single-file motion in either direction along the filter, as would be expected for a channel that does not show pronounced rectification under equilibrium simulation conditions. Also note that at  $\sim 1.9$  ns in KA02C ion K2 exits from the cavity through the intracellular gate, an event previously observed in KA13C (Shrivastava and Sansom, 2000).

In contrast, in NaA02C we started from the 2-ns configuration of NaA24C and repositioned Na3 at the extracellular mouth of the filter (i.e., similar to initial configuration of KA02C) and ran the simulation for 1.8 ns. From the trajectory it is evident that the  $Na^+$  fails to enter the filter and does not displace the water molecule at S1. Instead the external  $Na^+$  ion (Na3) moves close to site S0 where it is still able to retain part of its hydration shell. This contrasts with the situation in KA02C (see above) in which K3 enters the filter, apparently triggering further translocations.

#### NaA24C

As noted above, if the two  $Na^+$  ions in the filter were unrestrained during the equilibration period, they moved from S1 and S3 to S2 and S4 respectively before the



production run started. Thus, in simulation NaA24C the two  $\text{Na}^+$  ions were allowed to “relax” before starting the unrestrained simulation. In this case the two  $\text{Na}^+$  ions in the filter do not move at all over the period of the 2 ns simulation (data not shown). Na1 occupies a site close to S2, displaced toward S1 and Na2 occupies a site near S4, displaced toward S4.

Thus in the two KA simulations, three physiologically relevant phenomena have been observed: 1) single-file motion of  $\text{K}^+$  ions and water in both directions along the filter, 2) entry of a  $\text{K}^+$  ion into the selectivity filter at the extracellular mouth (as seen by Guidoni et al., 1999),; and 3) exit of  $\text{K}^+$  ion from the channel via the intracellular gate. Thus, it is evident that  $\text{K}^+$  ions are able to move along the KcsA channel on an  $\sim 2$ -ns timescale in these simulations.

In marked contrast, in none of the NaA simulations is there any concerted motion of  $\text{Na}^+$  ions and water along the filter, beyond fast initial relaxation of the system. Furthermore, from NaA02C it is evident that the  $\text{Na}^+$  does not enter the filter. This contrasts with the situation in KA02C (see above) in which K3 enters the filter, apparently triggering further translocations. Strikingly, throughout both NaA24C and NaA02C, ions Na1 and Na2 do not move. Again, this is in marked contrast with the  $\text{K}^+$  simulations. Thus, in these simulations  $\text{Na}^+$  differs from  $\text{K}^+$  in that 1) no concerted translocations of  $\text{Na}^+$  ions along the filter are seen, 2) entry of  $\text{Na}^+$  into the filter is not seen, and 3)  $\text{Na}^+$  does not interact with the carbonyl oxygens in the same way as  $\text{K}^+$ .

It might be argued that a small number of observed translocations of ions is statistically insignificant. Let us therefore summarize briefly the results of all the KA and NaA simulations, plus those in an earlier paper (Shrivastava and Sansom, 2000). Concerted translocations of  $\text{K}^+$  ions and water have been seen in all simulations with two or more ions in the filter. In contrast,  $\text{Na}^+$  ions have not been observed to move along the filter in NaA24C or NaA02C. In NaA13C there is an initial relaxation from the starting configuration but no further  $\text{Na}^+$  ion motion. Interestingly, if there is only a single  $\text{K}^+$  ion in the filter (simulations MDK1A and MDK1B in Shrivastava and Sansom, 2000) the ion does not move on a nanosecond timescale. Thus, we are reasonably confident of the differences we have observed between  $\text{K}^+$  and  $\text{Na}^+$  ions in these simulations. Of course, further and longer simulations would increase the statistical significance of our findings.

#### KB13C versus NaB13C

We also are aware of the difficulties of parameterization of  $\text{K}^+$  and  $\text{Na}^+$  ions (Tieleman et al., 2001). To explore this we ran simulations KB13C and NaB13C (Fig. 3), which used parameter set B, in which the van der Waals parameters for the two ions were similar to those of Åqvist (1990).

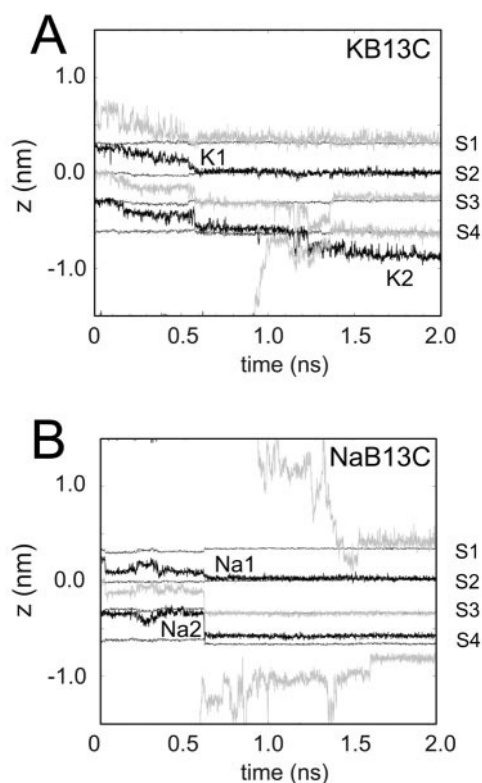


FIGURE 3 Trajectories (along the pore axis) of  $\text{K}^+$  or  $\text{Na}^+$  ions (black lines) and water molecules (gray lines) for simulations: (A) KB13C; (B) NaB13C. Other details are as for Fig. 2 except that zero on the  $z$  (pore axis) corresponds to the center of site S2.

In KB13C we see a concerted ion translocation event at  $\sim 0.5$  ns, and then at  $\sim 1.2$  ns the K2 ion leaves the filter, and so K-W-K in the filter is replaced by K-W-W (as was also seen in KA13C). In NaB13C there is an initial relaxation of the positions of the two  $\text{Na}^+$  ions, followed by no further movement of the ions along the filter. Again, the second ion, Na2, is displaced from the center of site S4 toward S3, as was seen in the simulations with sodium ions using parameter set A. Thus, small changes in the ionic parameters do not seem to qualitatively alter the behavior of  $\text{K}^+$  or  $\text{Na}^+$  ions in the filter.

#### Snapshots of the filter

A more structural insight into the difference between  $\text{K}^+$  and  $\text{Na}^+$  ions in the filter may be obtained by examining snapshots from the simulations (Fig. 4). For KA13C, snapshots are shown before and after a concerted translocation of the ion-water single file in the filter. At 200 ps, ions are at S1 and S3; by 400 ps they have moved to S2 and S4. At both times the  $\text{K}^+$  ions sit approximately in the centers of the sites, i.e., between the two rings of oxygen atoms. In contrast, in NaA24C, there is no change in the positions of the ions between the two snapshots (and, as we have seen

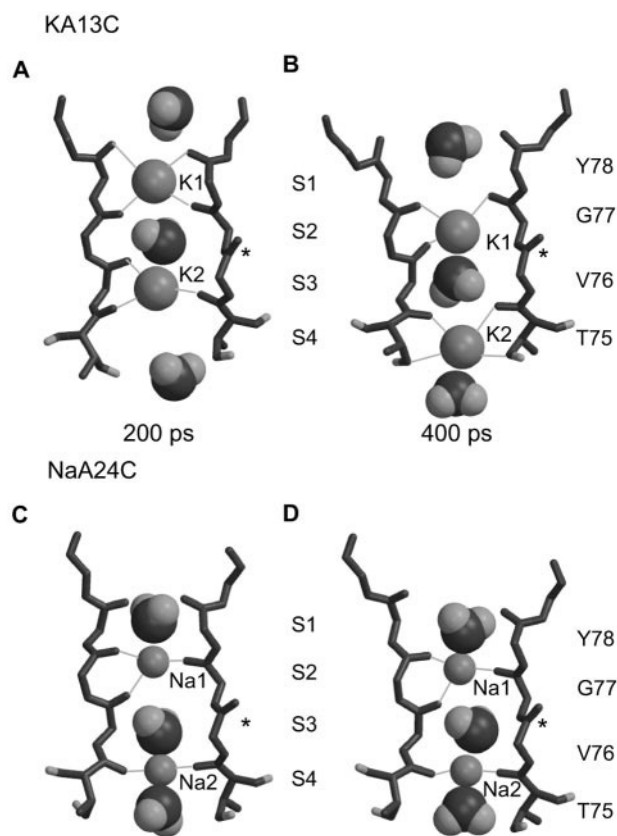


FIGURE 4 Snapshots of the selectivity filter (in bonds format) and ions plus selected waters (as van der Waals spheres) for KA13C (A and B) and NaA13C (C and D). In each case the snapshots are taken at 200 ps (A and C) and 400 ps (B and D). In the case of KA13C this is shortly before and after a concerted translocation of ions and water within the filter. The structure of the selectivity filter backbone is shown using two polypeptide chains out of the four. The asterisk indicates the V76-G77 peptide bond that has undergone a flip. Thin gray lines show oxygen/ion contacts.

above, no change occurs throughout the simulation). Limited motions of water molecules within the filter are seen, e.g., small changes in orientation of the two water molecules at sites S1 and S3. The other major difference between NaA24C and KA13C is between the interactions of ion and protein around S4. In KA13C at 400 ps the K2 ion sits in the center of S4, interacting with an upper ring of T75, carbonyl oxygens and a lower ring of T75, Oyl side-chain oxygens. In NaA24C, the Na2 ion sits exactly in the center of the T75, carbonyl oxygen ring. Thus, Na2 forms tight interactions with four carbonyl oxygens and the oxygen atoms of two water molecules (one at S3 and one just below the center of S4). This particular coordination geometry has not been seen for a  $K^+$  ion in the KcsA filter in our simulations. Significantly, in NaA13C, the Na1 ion also forms a tight interaction with just a single ring of carbonyl oxygens, in this case that of G77. Again, such an interaction has not been seen for  $K^+$ .

TABLE 2 Ionic configurations in the filter

Simulation	Initial configuration	Final configuration
KA13C	1010	0100
KA02C	0100	0010
KB13C	1010	0100
KA13Cp	1010	0101
KA024p	0101	0110
NaA13C	1010	0101 <sup>†</sup>
NaA02C	0101 <sup>†</sup>	0101 <sup>†</sup>
NaA24C	01 <sup>‡</sup> 01 <sup>†</sup>	01 <sup>‡</sup> 01 <sup>†</sup>
NaB13C	1010	0101 <sup>†</sup>
NaA13Cp	1010	1*010
NaA013p	1010	0101 <sup>†</sup>

Ionic configurations are indicated using the nomenclature introduced by Luzhkov and Åqvist (2000). Thus, 1010 indicates ions at sites S1 and S3, 0101 ions at sites S2 and S4, etc. For the  $Na^+$  simulations, 0101<sup>†</sup> indicates that the ion at site S4 is displaced towards site S3; 01<sup>‡</sup>01<sup>†</sup> indicates that the ion at site S2 is displaced towards site S1 and that at S4 is displaced towards S3. 1\*010 indicates that the ion at site S1 is displaced towards the extracellular mouth of the pore.

### Ionic configurations in the filter

The difference between the behavior of  $K^+$  and  $Na^+$  may be summarized by noting the configurations of ions in the filter at the start and end of the ~2-ns simulations (see Table 2), using the nomenclature of Åqvist and Luzhkov (2000) in which, e.g., 1010 indicates ions present at sites S1 and S3. From this summary it is evident that although 2 ns is sufficient time for  $K^+$  ions to translocate along the filter, and indeed to exit/enter the filter at either end, over the same time period  $Na^+$  ions relax from their initial configuration and then remain in the 0101 configuration, albeit with the ions displaced somewhat from the exact centers of the sites. If we take a figure of ~0.02 as an upper bound on the value  $P_{Na}/P_K$  (see above), then assuming translocation through the filter is proportional to this ratio, one might expect to have to run simulations of ~100-ns duration to see  $Na^+$  translocation events along the filter.

### Analysis of coordination numbers

A coordination number is defined as the number of ligands interacting with an ion. In a dynamic system, the coordination number is not a constant number, but varies with time. We have analyzed the number of O atoms (from the filter and from water molecules within the filter) coordinating the ions as a function of time (Fig. 5). In the present study, an O atom is considered to coordinate an ion if the distance of the O atom from the ion is less than 0.32 nm (for  $K^+$ ) or 0.27 nm (for  $Na^+$ ), based on data for ion/ligand interactions (reviewed in Tieleman et al., 2001).

In simulation KA13C, the coordination number of both  $K^+$  ions while in the filter is 8 or 9. Thus, K1 is coordinated by eight carbonyl oxygen atoms of residues Y78 and G77 and a water molecule. At ~500 ps, when the ion has moved

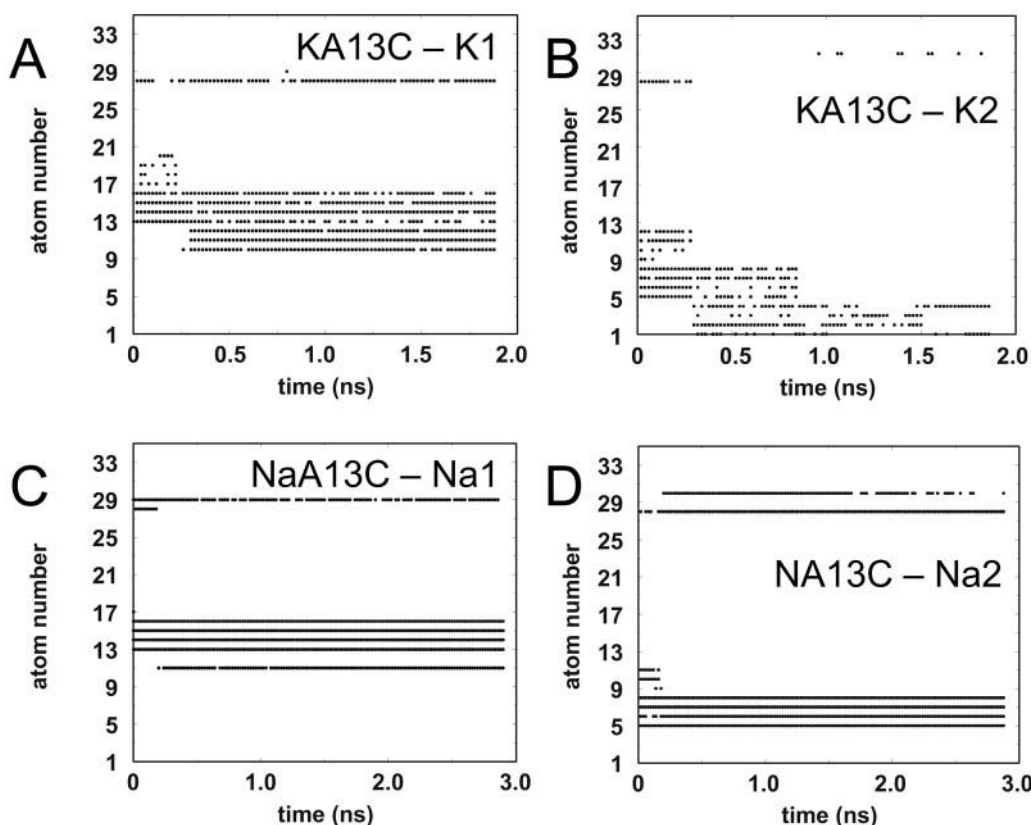


FIGURE 5 Ion coordination numbers versus time for simulations KA13C (K1 in *A*, K2 in *B*) and NaA13C (Na1 in *C*, Na2 in *D*). The numbers on the *y* axis correspond to the coordinating O atoms, such that numbers 1–4 are the side-chain oxygen atom of T75, whereas 5–8, 9–12, 13–16, 17–20, and 21–24 correspond to carbonyl oxygens of T75, V76, G77, Y78, and G79, respectively. The *y* values of 28 and above correspond to oxygen atoms of water molecules interacting with the ions. In particular, 28 is the oxygen atom of the water in between the ions K1 and K2 or Na1 and Na2 at the beginning of the simulation (see Fig. 1 *B*).

down, the coordinating atoms are G77 and three V76 (one of the V76 backbone oxygens has flipped away from the selectivity pore) and one water molecule. Thus the coordination number is 8. For K2, the coordinating atoms are the carbonyl oxygen atoms of V76 and T75 plus a water until ~250 ps. Thus the coordination number is again ~9. At 250 ps, when the ion has moved lower down into the filter, the coordinating atoms are the carbonyl and side-chain O atoms of T75, up to ~1 ns, at which point it goes into the cavity and is then coordinated by water molecules.

In contrast, analysis of the sodium ions, Na1 and Na2, in NaA13C reveals a constant coordination number of ~6. Na1 is coordinated with four G77 and one V76 carbonyl O, plus one water molecule, whereas the Na2 is coordinated with four T75 carbonyl O and two water molecules.

### Coordination geometry

The distances of the Na<sup>+</sup> ions from carbonyl O atoms of the selectivity filter residues in NaA24C clearly illustrate the tightness with which the Na<sup>+</sup> ions are bound. The mean Na-O distances are  $0.237 \pm 0.023$  nm at 200 ps and  $0.236 \pm$

$0.025$  nm at 400 ps, values closely comparable with  $0.235 \pm 0.003$  nm for Na-OH<sub>2</sub> distances in inorganic crystal hydrate structures (Hille, 1992) and within the range of distances (0.234–0.252 nm) for Na-O distances in a range of inorganic crystals (Tieleman et al., 2001). The fluctuation with respect to time of the Na-O distances in the simulations is very small (SD = 0.001 nm over 2 ns in NaA24C). Similar Na-O distances are seen for both Na1 and Na2 in NaA13C (0.223 and 0.225 nm, respectively). In contrast, the corresponding distances in the KA13C simulations are within the range for simple inorganic crystals ( $0.291 \pm 0.033$  nm at 200 ps and  $0.285 \pm 0.023$  nm at 400 ps), compared with 0.267–0.322 nm for K-O distances in inorganic crystals (Tieleman et al., 2001). The K-O distance seems to fluctuate more in the simulations, even in between translocations of the ions (SD = 0.01 nm over 0.9 ns in KA13C).

Of course, these differences are likely to be sensitive to parameterization of K-O and Na-O interactions. Accordingly, the ion parameters were examined by energy minimization (in vacuo) of a metal ion interacting with the carbonyl oxygen of an acetamide molecule and compared with results for energy minimization of an ion/water pair

(see Appendix). These test calculations revealed some sensitivity of the results to parameter set. Consequently, we have also compared ion-oxygen distances within the filter for simulations KB13C versus NaB13C, where the mean values are  $0.27 \pm 0.01$  nm and  $0.25 \pm 0.01$  nm, respectively. Thus, regardless of which parameter set is used,  $\text{Na}^+$  ions seem to bind tightly to the filter, in that the Na-O distance is within the range observed in inorganic crystal structures.

### Flexibility of the filter

It is evident even from a cursory examination of snapshots from a trajectory (Fig. 4) that the filter does not maintain a rigid geometry during the course of a simulation, but rather exhibits a degree of flexibility. Indeed, the dimensions of the selectivity filter pore are such that if it were rigid a  $\text{K}^+$  ion would not be free to pass through it (minimum radius of the filter  $\sim 0.085$  nm vs.  $0.133$  nm for the ionic radius of  $\text{K}^+$ ). However, it is also evident that the filter is not completely deformable. Examination of the filter during simulations reveals three types of distortion from the x-ray structure. First, there are relatively small ( $\sim 0.1$  nm) movements of carbonyl groups, often coupled to ion translocation so as to optimize ion-carbonyl and water-carbonyl interactions. These are revealed by, e.g., comparing O-O distances across the pore in the x-ray structure with those in the simulation snapshots. For example, the O-O distances in the x-ray model are 0.596, 0.440, 0.470, 0.548, and 0.618 nm for Y78, CO; G77, CO; V76, CO; T75, CO; and T75, O $\gamma$ , respectively. In the 200-ps snapshot of KA13C they are 0.478, 0.447, 0.523, 0.520, and 0.655 nm; in the 400-ps snapshot they are 0.643, 0.442, 0.432, 0.418, and 0.562 nm. These small changes ( $\sim 0.05$  nm) are typical of other simulations (e.g., NaA13C). In the simulations with parameter set B (KB13C and NaB13C) also, the changes in the O-O distances are of a similar order of magnitude.

Analysis of the pore radius profiles for the filter region of the channel during the simulations reveals significant differences between the  $\text{K}^+$  and  $\text{Na}^+$  simulations. In all cases, the rings of oxygen atoms that line the filter constrict it to a radius less than that of a  $\text{K}^+$  ion, as is the case in the x-ray structure. However, comparing filter radius profiles for, e.g., KA13C with those of NaA24C (Fig. 6) reveals a degree of contraction of the filter to accommodate the smaller  $\text{Na}^+$  ions. Thus, in KA13C the average radius in the filter is generally above 0.1 nm, whereas for NaA24C it falls to  $\sim 0.05$  nm in places. Pore radius profiles for KB13C and NaB13C reveal a similar difference. Thus the filter clearly is distortable by the ions once they are within it, and the distortion is significantly greater when the filter is occupied by  $\text{Na}^+$  ions.

Second, peptide bond flips, such as that seen in Fig. 4, appear to be associated with ion translocation. This flip is always associated with the peptide bond between V76 and

G77 (as also been seen by Bernèche and Roux, 2000). In particular, we have seen this peptide flip in V76/G77 of one subunit in simulations KA13C, NaA13C, KB13C, and NaB13C, but not in NaA24C. In the simulations described in a previous study (Shrivastava and Sansom, 2000) the peptide flip was seen in simulations with two  $\text{K}^+$  ions in the channel (which showed ion translocation through the filter) but not in simulations with a single  $\text{K}^+$  ion (which did not translocate), although this was not reported in the earlier paper. Note that in all of our simulations the V76/G77 peptide has not flipped at  $t = 0$ . Thus, flipping of this peptide bond seems to be associated with ion/water movement in the filter. The flipping of this peptide, results in creating a space in the selectivity filter, through which a water molecule can squeeze past the  $\text{K}^+$  ion, thus changing a K-W-K single file to K-W-W-K single file mentioned above.

Third, there are changes in the pattern of H-bonding between the tyrosine side chains (Y78) of the TVGYG motif and the tryptophan side chains (W67) from the surrounding P-helices. The latter H-bonding interactions were suggested by Doyle et al. (1998) to help stabilize the conformation of the filter, thus providing an optimal fit of the latter with  $\text{K}^+$  ions. Interestingly, if one compares this tyrosine-tryptophan interaction for KA13C and NaA24C at, e.g., 400 ps (Fig. 7), these interactions are more or less maintained in KA13C, but two of the four tyrosine side chains have changed their conformations in NaA24C such that the hydrogen-bonding interactions are not retained. Another hydrogen-bonding interaction helping to maintain the conformation of the selectivity filter is between the aromatic residues Y78 and W67 and residue E71, which is a part of the P-loop helix, with its side chain extending out between the helix and the TVGYG filter motif. The two hydrogen bonds (E71-Y78) and (E71-W67), in which the carboxyl side chain interacts with backbone NH, are maintained throughout the simulation in NaA13C, whereas in KA13C, the bonds are not so rigorously maintained. Thus, the interactions of E71 in the simulations with  $\text{Na}^+$  ions is more or less constant throughout the simulation, possibly lending more rigidity to the selectivity filter as compared with the simulation with  $\text{K}^+$  ions.

### Changing the Glu71/Asp80 ionization state

In the simulations discussed so far all protein side chains have been assumed to be in their default ionization states. In particular, all Asp and Glu side chains have been assumed to be fully ionized. However, on the basis of careful examination of the x-ray structure (reported in Bernèche and Roux, 2000; Roux et al., 2000) and on the basis of  $\text{pK}_A$  calculations (Ranatunga et al., 2001; Luzhkov and Åqvist, 2000; Bernèche and Roux, 2002) it has been suggested that the Glu71/Asp80 side-chain pair in each subunit is not fully ionized, but rather that each Glu71/Asp80 pair shares a



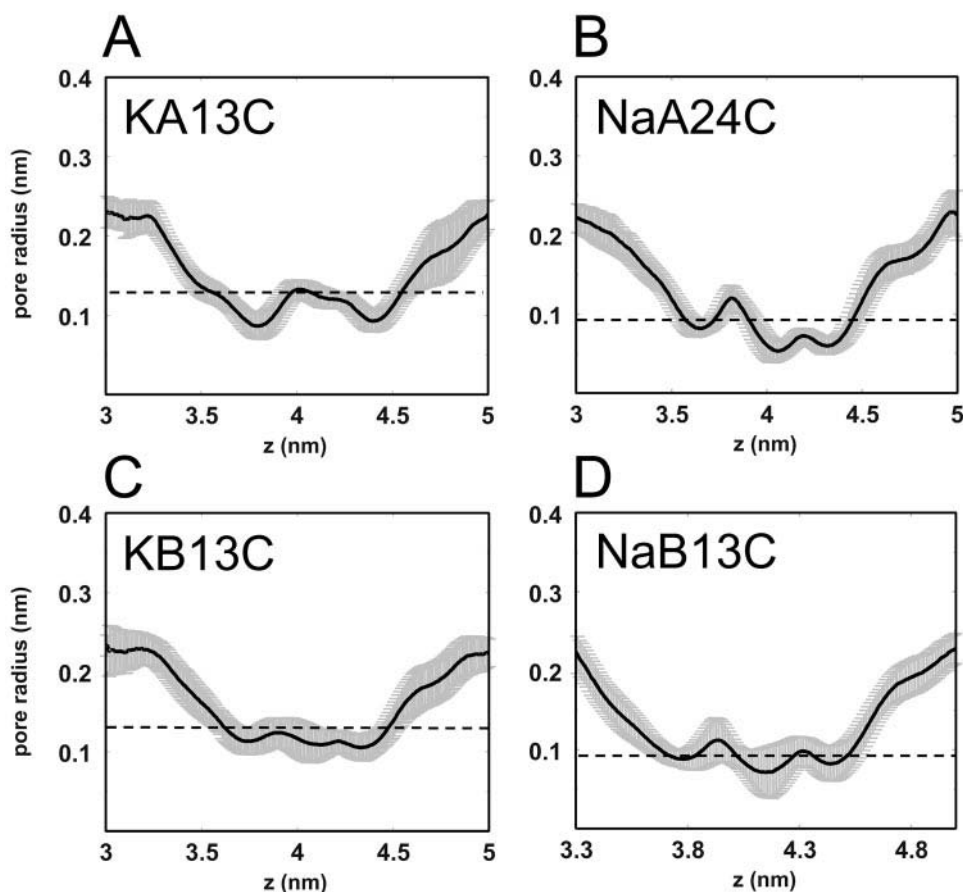


FIGURE 6 Pore radius profiles (evaluated using HOLE (Smart et al., 1993)) compared for the filter regions of simulations: (A) KA13C; (B) NaA24C; (C) KB13C; (D) NaB13C. The cavity end of the filter is at  $z \approx 3$  nm and the extracellular mouth at  $z \approx 5$  nm. Each profile corresponds to the time-averaged pore radius profile over the entire simulation period (solid black line) with the error bars showing  $\pm$ SD (gray). The dotted horizontal lines indicate the ionic radii of  $K^+$  and  $Na^+$  ions for their respective simulations.

single proton, i.e., carries a net charge of  $-1e$ . This is also suggested by the more recent higher-resolution x-ray structure of KcsA (Zhou et al., 2001). The possible influence of this on the simulation results has been explored in simulations KA13Cp, KA024p, NaA13Cp, and NaA013p (see Table 1). The initial configuration of KA13Cp and of NaA13Cp is the same as those of their fully ionized equivalents KA13C and NaA13C, respectively. The initial configuration of simulation KA024p was obtained by taking the  $t = 2$  ns configuration of KA13Cp and moving the cavity  $K^+$  ion (which had exited from the channel through the intracellular mouth) and placing it just outside site S0, i.e., in the extracellular mouth of the channel. The initial configuration of NaA013p was derived from the  $t = 2$  ns configuration of NaA13C in a similar fashion.

In terms of overall ion movements the results of the ‘p’ simulations are quite similar to those of the fully ionized simulations (see Table 2). For example in both KA13C and KA13Cp the ions initially at sites S1 and S3 move to sites S2 and S4. In contrast, with the sodium ion simulations, in both NaA13C and NaA13Cp the ions undergo some initial

relaxation followed by no further translocation through the selectivity filter. Similarly, in both simulations KA02C and KA024p the  $K^+$  ion placed at the external mouth of the channel enters the selectivity filter and moves along it, whereas in both NaA02C and NaA013Cp the  $Na^+$  ion in the external mouth fails to enter the filter, but sits close to site S0.

Comparison of the pore radius profiles for, e.g., simulations KA13C and KA13Cp reveals no significant differences in the profiles in the vicinity of the filter. Thus, we feel it is safe to conclude, at least to a first level of approximation, that the change in the ionization state of Glu71/Asp80 does not have a major effect on the geometry of the filter per se in our simulations.

We have also examined coordination numbers of the  $K^+$  and  $Na^+$  ions while within the filter during the ‘p’ simulations. For the  $K^+$  ions within the filter, the coordination numbers range from 6 to 9 dependent on the exact configuration of the system. In contrast, for the  $Na^+$  ions in the filter the coordination numbers are generally 5 or 6, although in one case (the  $Na^+$  ion at site S3 in NaA13Cp) this rises to  $\sim 8$ .

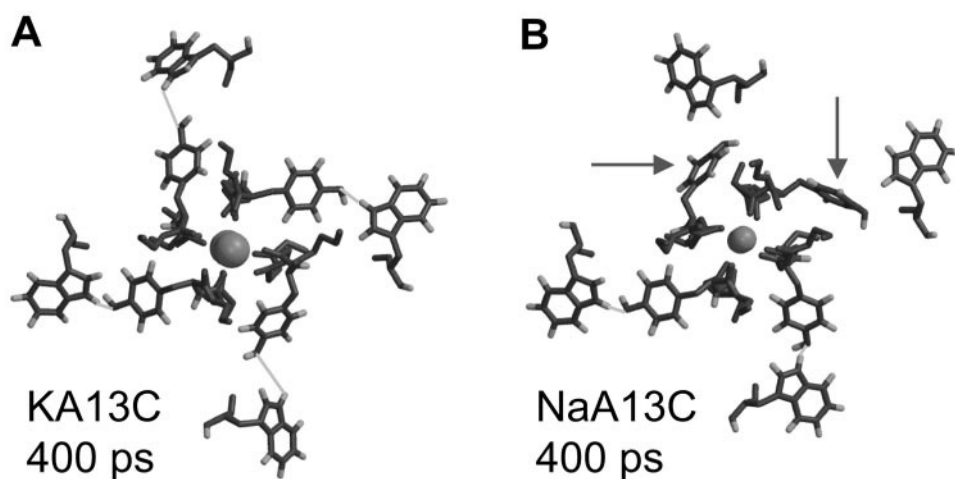


FIGURE 7 Snapshots of the aromatic side chains surrounding the selectivity filter (Y78 and W68) for KA13C (*A*) and NaA24C (*B*), both at 400 ps. The backbone atoms of the filter and the  $K^+$  or  $Na^+$  ions are also shown, and the view is down the pore axis. (*B*) It is evident that changes in the conformation of two Y78 side chains have occurred (*arrows*) and that the carbonyl oxygen rings have contracted about the central  $Na^+$  ions.

Thus, on balance, we conclude that the difference in ionization state (Glu71/Asp80 fully ionized versus the same side-chain pair sharing a proton) does not have a profound effect on the simulation results with respect to the difference in behavior of  $K^+$  versus  $Na^+$  ions in the filter. At first this is perhaps a little puzzling as one might expect the difference in side-chain ionization states (and hence in side-chain configuration (Ranatunga et al., 2001)) might result in a difference in flexibility of the selectivity filter. However, careful inspection of the simulations reveals that, for example, in simulation KA13C a Glu71 side-chain to Asp80 main-chain H-bond fixes the position of the Glu71 side chain (and hence contributes to the conformation of the filter), thus effectively playing a similar role to the G71 side-chain to Asp80 side-chain H-bond in simulation KA13Cp.

## DISCUSSION

### Biological significance

Are these simulation results of biological significance? It is known that KcsA is selective for  $K^+$  over  $Na^+$  ions and that internal  $Na^+$  ions can block the channel (Heginbotham et al., 1999; LeMasurier et al., 2000). These properties are typical of other K channels, including Kv channels (Hille, 1992). As discussed above, a number of studies on animal K channels (French and Wells, 1977; Korn and Ikeda, 1995; Kiss et al., 1998; Immke et al., 1999; Loboda et al., 2001; Heginbotham et al., 1994; Proks et al., 2001) suggest that  $Na^+$  ions may enter the selectivity filter of various K channels, albeit with a much lower probability than for  $K^+$ .

It is encouraging that in our simulations  $K^+$  ions undergo concerted single-file motions (in either direction; see KA02C at  $t = 1.55$  ns, Fig. 2 *B*) along the filter. In contrast,

$Na^+$  ions bind to the filter and do not undergo sustained single-file motion along the filter on a 2-ns timescale, although some initial relaxation may occur. Furthermore, an extracellular  $Na^+$  ion placed at the mouth of the pore does not enter the filter whereas a  $K^+$  ion in the same location does enter, on a nanosecond timescale (as was also seen in simulations by Guidoni et al., 1999). Thus the simulations seem to reproduce aspects of an essential feature of K channel physiology, i.e., selection for  $K^+$  over  $Na^+$ .

What is the physical origin of ion selectivity in KcsA, whereby  $K^+$  ions can permeate the selectivity filter whereas  $Na^+$  ions bind and block? It seems to lie in a subtle balance of rigidity and flexibility created by the channel protein structure. Thus,  $K^+$  ions sit within the sites created by rings of eight O atoms, with some local distortion (see below), whereas  $Na^+$  ions are small enough to fit into the center of a ring of four O atoms. If single  $K^+$  ions are bound within the filter, they do not permeate (at least on a nanosecond timescale (Shrivastava and Sansom, 2000)). However, the presence of multiple  $K^+$  ions in the filter sufficiently destabilizes interactions to enable permeation, as suggested by Doyle et al. (1998). This picture of permeation and selectivity is perhaps more subtle than that formulated in terms of a rigid selectivity filter. Analysis of changes in the radius profile between different simulations supports the model of a deformable filter.

It is important to compare our picture of selectivity with that of Åqvist and Luzhkov (2000), who employed free energy perturbation calculations to explore the relative free energies of different configurations of  $K^+$  ions in the selectivity filter sites (S1 to S4) and, for the most stable configuration of  $K^+$  ions, to calculate the free energy cost of mutating two  $K^+$  ions to two  $Na^+$  ions. It is encouraging that they estimate the most stable configuration of two  $K^+$

ions in the filter to be 0101, which in our nomenclature corresponds to K1 at S2 and K2 at S4, as this configuration also appears to be the most stable in both our current and earlier (Shrivastava and Sansom, 2000) publications. In terms of selectivity, Åqvist and Luzhkov (2000) mutated K1 (at S2) and K2 (at S4) to Na1 (at S2) and Na2 (at S4) and show that the increase in binding free energy is  $\sim +8$  kJ mol<sup>-1</sup>. However, as the current simulations show, these are not the preferred binding sites for Na<sup>+</sup> ions, which prefer to move to just above S2 and S4 to optimize their interactions with the selectivity filter. During the ion mutation calculations (Åqvist and Luzhkov, 2000) the ions were restrained to remain at sites S2 and S4. Thus, our simulations emphasize the importance of performing unrestrained simulations to more fully explore ion/filter/water dynamics. In particular, we suggest that small movements of the Na<sup>+</sup> ions in the filter allow relaxation to a blocked state that must be considered if simulations are to correctly explain the physiological observations.

It is also of interest that our simulations reveal flexibility of the filter. This has also been seen in other simulations of KcsA (Guidoni et al., 1999; Bernèche and Roux, 2000) that have employed different MD codes and energy function parameters, and also in simulations of models of the more distantly related Kir channels (Hu et al., 2000; Capener and Sansom, 2002). Thus, a consensus seems to be emerging from simulations that the filter is not rigid but rather is deformable by K<sup>+</sup> and by Na<sup>+</sup> ions. For K<sup>+</sup> such deformability is associated with ion permeation. For Na<sup>+</sup> ions the deformability is seen as a local constriction of a ring of carbonyl groups about a blocking Na<sup>+</sup> ion. Thus, filter flexibility enables larger ions (K<sup>+</sup> and Rb<sup>+</sup>) to squeeze through the filter while at the same time enabling smaller ions (e.g., Na<sup>+</sup>) to block by condensation of the filter around them. We note that recent physiological studies of K<sup>+</sup> channels (Yang et al., 2000) have demonstrated the existence of sub-conductance levels that have been suggested to reflect small conformational changes in the selectivity filter region.

We note that in some simulations we observe a transition that yields just a single K<sup>+</sup> ion in the filter. For example, this can be seen for simulations KA13C and KA13B at  $\sim 2$  ns. The K<sup>+</sup> ion sits at site S2 with water molecules at both S3 and S4. We note that, in the recent higher-resolution x-ray structure, K<sup>+</sup> ions appear to be able to occupy all four sites (S1 to S4) with approximately equal probability. However, in the average picture seen in an x-ray structure it would be difficult to exclude a low probability of occupation of some sites by water, thus yielding some single K<sup>+</sup> ion configurations. Further work is needed to resolve this.

### Limitations of current simulations

There are a number of technical issues with respect to the current simulations. These include the use of cutoffs to

truncate long-range (i.e.,  $>1.7$  nm) electrostatic interactions rather than Ewald summation (Tieleman et al., 1997) and the relatively low (0.32 nm) resolution of the starting structure, along with the absence of the N- and C-terminal tails from the KcsA model (Doyle et al., 1998). All of these aspects merit systematic investigation, but our preliminary tests (Shrivastava, Capener, and Sansom, unpublished results; Capener and Sansom, 2002) leave us confident that our conclusions will not change qualitatively on the basis of a different treatment of such factors. Furthermore, in terms of comparing the two species of ions, it might be expected that the errors would be similar for the two sets of simulations and so are likely to cancel.

Another limitation of the simulations is that of parameters used for ion/filter and ion/water interactions. As discussed in the context of gramicidin (Roux and Karplus, 1991, 1994) even with nonpolarizable models, careful consideration of such interactions is essential. We are encouraged that our results seem to be robust to small changes in ion parameters. However, in terms of accurate treatment of the energetics of K<sup>+</sup> versus Na<sup>+</sup> it seems likely that some treatment of electronic polarization (Guidoni and Carloni, 2001) may be necessary.

Another important question one must address is that of timescales. Our simulations are all of length  $\sim 2$  ns. The translocation of K<sup>+</sup> ions between sites occurs on an  $\sim 0.5$ -ns timescale. From the single-channel conductance of KcsA we estimate a mean passage time of a K<sup>+</sup> ion through the channel of  $\sim 20$  ns, i.e., approximately an order of magnitude greater than the timescale of translocation within the filter. Are these two figures consistent? First, one should remember that several translocation events will be required for an ion to fully traverse the filter. Second, the ion has to enter the filter. Simulations by Guidoni et al. (1999) and by us (KA02C) suggest that this takes place on a similar timescale to that for site-to-site translocation. Furthermore, the ratio of downwards (i.e., extracellular  $\rightarrow$  intracellular) to upwards (i.e., intracellular  $\rightarrow$  extracellular) translocations will be determined by inter alia the voltage difference across the channel (which is not included in the current simulation, which corresponds to a KcsA channel at equilibrium). Finally, it should be remembered that the x-ray structure of KcsA may correspond more closely to the closed structure of the channel and that changes in the pore dimensions at the intracellular mouth of the channel (the gate in Fig. 1) are needed to allow ion exit/entry from/to the central cavity (Perozo et al., 1999). As entry/exit of ions through the gate is a rare event in simulations its timescale is difficult to determine. This event has been seen three times in  $\sim 10$  ns of KcsA simulations with three K<sup>+</sup> ions present (Shrivastava and Sansom, 2002). This gives a lower bound of  $\sim 5$  ns for the mean passage time in simulations, which is in reasonable agreement with the experimental estimate. Further, longer, simulations are needed to explore this in more detail. However, it is evident that the timescales of translo-

**TABLE 3** Ionic parameters

Parameters	Na <sup>+</sup>		K <sup>+</sup>	
	$\epsilon$	$R_{\text{MIN}}/2$	$\epsilon$	$R_{\text{MIN}}/2$
Set A	-0.0148	0.14453	-0.00001353	0.36227
Set B	-0.00084498	0.20638	-0.000328	0.27695

$\epsilon$  (kcal mol<sup>-1</sup>) is the depth of the energy well in the van der Waals interaction and  $R_{\text{MIN}}$  (nm) the point at which  $U = 0$ .

cation of K<sup>+</sup> ions in the filter seen in the current study are reasonable. As discussed above, we estimate that we would need to run simulations for at least 100 ns to see Na<sup>+</sup> translocation.

In summary, three conclusions emerge from our simulations. 1) Simulations of KcsA in a bilayer correlate with the experimentally observed selectivity of the channel for K<sup>+</sup> over Na<sup>+</sup> ions. 2) K<sup>+</sup> ions appear to translocate between sites within the selectivity filter on a nanosecond timescale, whereas on the same timescale Na<sup>+</sup> ions remain bound within the filter. 3) The selectivity filter exhibits a degree of flexibility, and the exact nature of the conformational changes undergone is important in allowing the channel to discriminate between permeant and blocking ions.

## APPENDIX

### Na<sup>+</sup> and K<sup>+</sup> parameters

The aim of the present study is to explore the nature of ion selectivity of a K channel. To test the robustness of the simulation results to ion parameter, we decided to use two sets of interaction parameters for the ions (Table 3). In parameter set A the K<sup>+</sup> and Na<sup>+</sup> parameters were as in Straatsma and Berendsen (1988). Set B employed parameters derived from those in Åqvist (1990) for use in Gromacs. For each model, both K<sup>+</sup> and Na<sup>+</sup>, two energy minimizations were performed: of an ion/acetamide pair, the carbonyl oxygen of *N*-methylacetamide interacting with the cation; and for an ion/water pair. SPC water was used and *N*-methylacetamide parameters were from the standard Gromacs/Gromos distribution. The results are reported in Table 4. It is evident that there is some sensitivity of the results to parameters, but a consensus of 0.22–0.23 nm for the Na/O distance vs. 0.27–0.28 nm for the K/O distance emerges. These are similar to the distances seen for interactions within the selectivity filter in our simulations.

**TABLE 4** Interactions with SPC water and with *N*-Me-acetamide

Parameters	Na <sup>+</sup>				K <sup>+</sup>			
	Water		<i>N</i> -Me-acetamide		Water		<i>N</i> -Me-acetamide	
	R	U	R	U	R	U	R	U
Set A	0.2174	-29.60	0.2121	-25.93	0.2851	-18.04	0.2837	-16.93
Set B	0.2333	-25.88	0.2298	-22.92	0.2716	-19.74	0.2686	-18.40

$R$  is the ion/oxygen distance (nm) and  $U$  is the interaction energy after minimization (kcal mol<sup>-1</sup>).

Our thanks to all of our colleagues, especially Declan Doyle, Kishani Ranatunga, and Graham Smith, for helpful discussions.

This work was supported by grants from The Wellcome Trust (to M.S.P.S. and to P.C.B.), and additional computer time was provided by the Oxford Supercomputing Center. D.P.T. was supported by an EMBO fellowship and is an AHFMR Scholar.

## REFERENCES

- Allen, T. W., A. Bliznyuk, A. P. Rendell, S. Kuyucak, and S. H. Chung. 2000. The potassium channel: structure, selectivity and diffusion. *J. Chem. Phys.* 112:8191–8204.
- Allen, T. W., S. Kuyucak, and S. H. Chung. 1999. Molecular dynamics study of the KcsA potassium channel. *Biophys. J.* 77:2502–2516.
- Åqvist, J. 1990. Ion water interaction potentials derived from free-energy perturbation simulations. *J. Phys. Chem.* 94:8021–8024.
- Åqvist, J., and V. Luzhkov. 2000. Ion permeation mechanism of the potassium channel. *Nature*. 404:881–884.
- Armstrong, C. M. 1998. The vision of the pore. *Science*. 280:56–57.
- Ashcroft, F. M. 2000. *Ion Channels and Disease*. Academic Press, San Diego.
- Berendsen, H. J. C., J. P. M. Postma, W. F. van Gunsteren, A. DiNola, and J. R. Haak. 1984. Molecular dynamics with coupling to an external bath. *J. Chem. Phys.* 81:3684–3690.
- Berendsen, H. J. C., J. P. M. Postma, W. F. van Gunsteren, and J. Hermans. 1981. *Intermolecular Forces*. Reidel, Dordrecht, Germany.
- Berger, O., O. Edholm, and F. Jahnig. 1997. Molecular dynamics simulations of a fluid bilayer of dipalmitoylphosphatidylcholine at full hydration, constant pressure and constant temperature. *Biophys. J.* 72:2002–2013.
- Bernèche, S., and B. Roux. 2000. Molecular dynamics of the KcsA K<sup>+</sup> channel in a bilayer membrane. *Biophys. J.* 78:2900–2917.
- Bernèche, S., and B. Roux. 2001. Energetics of ion conduction through the K<sup>+</sup> channel. *Nature*. 414:73–77.
- Bernèche, S., and B. Roux. 2002. The ionization state and the conformation of Glu-71 in the KcsA K<sup>+</sup> channel. *Biophys. J.* 82:772–780.
- Biggin, P. C., G. R. Smith, I. H. Shrivastava, S. Choe, and M. S. P. Sansom. 2001. Potassium and sodium ions in a potassium channel studied by molecular dynamics simulations. *Biochim. Biophys. Acta*. 1510:1–9.
- Capener, C. E., and M. S. P. Sansom. 2002. MD Simulations of a K channel model: sensitivity to changes in ions, waters and membrane environment. *J. Phys. Chem. B*. 106:4543–4551.
- Capener, C. E., I. H. Shrivastava, K. M. Ranatunga, L. R. Forrest, G. R. Smith, and M. S. P. Sansom. 2000. Homology modeling and molecular dynamics simulation studies of an inward rectifier potassium channel. *Biophys. J.* 78:2929–2942.
- Chang, G., R. H. Spencer, A. T. Lee, M. T. Barclay, and D. C. Rees. 1998. Structure of the MscL homolog from *Mycobacterium tuberculosis*: a gated mechanosensitive ion channel. *Science*. 282:2220–2226.
- Chung, S. H., T. W. Allen, and S. Kuyucak. 2002. Conducting-state properties of the KcsA potassium channel from molecular and Brownian dynamics simulations. *Biophys. J.* 82:628–645.
- Darden, T., D. York, and L. Pedersen. 1993. Particle mesh Ewald: an N.log(N) method for Ewald sums in large systems. *J. Chem. Phys.* 98:10089–10092.
- Doyle, D. A., J. M. Cabral, R. A. Pfuetzner, A. Kuo, J. M. Gulbis, S. L. Cohen, B. T. Cahit, and R. MacKinnon. 1998. The structure of the potassium channel: molecular basis of K<sup>+</sup> conduction and selectivity. *Science*. 280:69–77.
- Forrest, L. R., and M. S. P. Sansom. 2000. Membrane simulations: bigger and better? *Curr. Opin. Struct. Biol.* 10:174–181.
- French, R. J., and J. B. Wells. 1977. Sodium ions as blocking agents and charge carriers in the potassium channel of squid giant axon. *J. Gen. Physiol.* 70:707–724.



- Guidoni, L., and P. Carloni. 2002. Potassium permeation through the KcsA channel: a density functional study. *Biochim. Biophys. Acta*. 1563:1–6.
- Guidoni, L., V. Torre, and P. Carloni. 1999. Potassium and sodium binding in the outer mouth of the K<sup>+</sup> channel. *Biochemistry*. 38:8599–8604.
- Heginbotham, L., M. LeMasurier, L. Kolmakova-Partensky, and C. Miller. 1999. Single *Streptomyces lividans* K<sup>+</sup> channels: functional asymmetries and sidedness of proton activation. *J. Gen. Physiol.* 114:551–559.
- Heginbotham, L., Z. Lu, T. Abramsom, and R. MacKinnon. 1994. Mutations in the K<sup>+</sup> channel signature sequence. *Biophys. J.* 66:1061–1067.
- Hess, B., H. Bekker, H. J. C. Berendsen, and J. G. E. M. Fraaije. 1997. LINCS: a linear constraint solver for molecular simulations. *J. Comp. Chem.* 18:1463–1472.
- Hille, B. 1992. *Ionic Channels of Excitable Membranes*. Sinauer Associates, Sunderland, MA.
- Hu, J., S. Goldman, C. G. Gray, and H. R. Guy. 2000. Calculation of the conductance and selectivity of an ion-selective potassium channel (IRK1) from simulation of atomic scale models. *Mol. Phys.* 98:535–547.
- Immke, D., M. Wood, L. Kiss, and S. J. Korn. 1999. Potassium-dependent changes in the conformation of the Kv2.1 potassium channel pore. *J. Gen. Physiol.* 113:819–836.
- Kiss, L., D. Immke, J. LoTurco, and S. J. Korn. 1998. The interaction of Na<sup>+</sup> and K<sup>+</sup> in voltage-gated potassium channels: evidence for cation binding sites of different affinity. *J. Gen. Physiol.* 111:195–206.
- Korn, S. J., and S. R. Ikeda. 1995. Permeation selectivity by competition in a delayed rectifier potassium channel. *Science*. 269:410–412.
- Kraulis, P. J. 1991. MOLSCRIPT: a program to produce both detailed and schematic plots of protein structures. *J. Appl. Crystallogr.* 24:946–950.
- LeMasurier, M., L. Heginbotham, L. Kolmakova-Partensky, and C. Miller. 2000. Selectivity properties of the KcsA K<sup>+</sup> channel. *Biophys. J.* 78:398a. (Abstr.)
- LeMasurier, M., L. Heginbotham, and C. Miller. 2001. KcsA: it's a potassium channel. *J. Gen. Physiol.* 118:303–313.
- Loboda, A., A. Melishchuk, and C. Armstrong. 2001. Dilated and defunct K channels in the absence of K<sup>+</sup>. *Biophys. J.* 80:2704–2714.
- Lü, Q., and C. Miller. 1995. Silver as a probe of pore-forming residues in a potassium channel. *Science*. 268:304–307.
- Luzhkov, V. B., and J. Åqvist. 2000. A computational study of ion binding and protonation states in the KcsA potassium channel. *Biochim. Biophys. Acta*. 1481:360–370.
- MacKinnon, R., S. L. Cohen, A. Kuo, A. Lee, and B. T. Chait. 1998. Structural conservation in prokaryotic and eukaryotic potassium channels. *Science*. 280:106–109.
- Marrink, S. J., O. Berger, D. P. Tieleman, and F. Jahnig. 1998. Adhesion forces of lipids in a phospholipid membrane studied by molecular dynamics simulations. *Biophys. J.* 74:931–943.
- Merritt, E. A., and D. J. Bacon. 1997. Raster3D: photorealistic molecular graphics. *Methods Enzymol.* 277:505–524.
- Meuser, D., H. Splitt, R. Wagner, and H. Schrempf. 1999. Exploring the open pore of the potassium channel from *Streptomyces lividans*. *FEBS Lett.* 462:447–452.
- Miller, C. 1991. 1990: Annus mirabilis of potassium channels. *Science*. 252:1092–1096.
- Nimigean, C. M., and C. Miller. 2002. Na block and permeation in single KcsA K channels. *Biophys. J.* 82:350a. (Abstr.)
- Perozo, E., D. M. Cortes, and L. G. Cuello. 1999. Structural rearrangements underlying K<sup>+</sup>-channel activation gating. *Science*. 285:73–78.
- Pinto, L. H., G. R. Dieckmann, C. S. Gandhi, C. G. Papworth, J. Braman, M. A. Shaughnessy, J. D. Lear, R. A. Lamb, and W. F. DeGrado. 1997. A functionally defined model for the M<sub>2</sub> proton channel of influenza A virus suggest a mechanism for its ion selectivity. *Proc. Natl. Acad. Sci. U.S.A.* 94:11301–11306.
- Plugge, B., S. Gazzarrini, M. Nelson, R. Cerana, J. L. Van Etten, C. Derst, D. DiFrancesco, A. Moroni, and G. Thie. 2000. A potassium channel protein encoded by chlorella virus PBCV-1. *Science*. 287:1641–1644.
- Proks, P., C. E. Capener, P. Jones, and F. Ashcroft. 2001. Mutations within the P-loop of Kir6.2 modulate the intraburst kinetics of the ATP-sensitive potassium channel. *J. Gen. Physiol.* 118:341–353.
- Ranatunga, K. M., I. H. Shrivastava, G. R. Smith, and M. S. P. Sansom. 2001. Side-chain ionization states in a potassium channel. *Biophys. J.* 80:1210–1219.
- Randa, H. S., L. R. Forrest, G. A. Voth, and M. S. P. Sansom. 1999. Molecular dynamics of synthetic leucine-serine ion channels in a phospholipid membrane. *Biophys. J.* 77:2400–2410.
- Roux, B., S. Bernèche, and W. Im. 2000. Ion channels, permeation and electrostatics: insight into the function of KcsA. *Biochemistry*. 39:13295–13306.
- Roux, B., and M. Karplus. 1991. Ion transport in a model gramicidin channel: structure and thermodynamics. *Biophys. J.* 59:961–981.
- Roux, B., and M. Karplus. 1994. Molecular dynamics simulations of the gramicidin channel. *Annu. Rev. Biophys. Biomol. Struct.* 23:731–761.
- Roux, B., and R. MacKinnon. 1999. The cavity and pore helices in the KcsA K<sup>+</sup> channel: electrostatic stabilization of monovalent cations. *Science*. 285:100–102.
- Sansom, M. S. P., I. H. Shrivastava, K. M. Ranatunga, and G. R. Smith. 2000. Simulations of ion channels: watching ions and water move. *Trends Biochem. Sci.* 25:368–374.
- Schrempf, H., O. Schmidt, R. Kummerlein, S. Hinnah, D. Muller, M. Betzler, T. Steinkamp, and R. Wagner. 1995. A prokaryotic potassium-ion channel with 2 predicted transmembrane segments from *Streptomyces lividans*. *EMBO J.* 14:5170–5178.
- Shrivastava, I. H., and M. S. P. Sansom. 2000. Simulations of ion permeation through a potassium channel: molecular dynamics of KcsA in a phospholipid bilayer. *Biophys. J.* 78:557–570.
- Shrivastava, I. H., and M. S. P. Sansom. 2002. Molecular dynamics simulations and KcsA channel gating. *Eur. Biophys. J.* 31:207–216.
- Smart, O. S., J. M. Goodfellow, and B. A. Wallace. 1993. The pore dimensions of gramicidin A. *Biophys. J.* 65:2455–2460.
- Straatsma, T. P., and H. J. C. Berendsen. 1988. Free-energy of ionic hydration: analysis of a thermodynamic integration technique to evaluate free-energy differences by molecular-dynamics simulations. *J. Chem. Phys.* 89:5876–5886.
- Tieleman, D. P., and H. J. C. Berendsen. 1998. A molecular dynamics study of the pores formed by *Escherichia coli* OmpF porin in a fully hydrated palmitoylcholine bilayer. *Biophys. J.* 74:2786–2801.
- Tieleman, D. P., H. J. C. Berendsen, and M. S. P. Sansom. 1999. An alamethicin channel in a lipid bilayer: molecular dynamics simulations. *Biophys. J.* 76:1757–1769.
- Tieleman, D. P., P. C. Biggin, G. R. Smith, and M. S. P. Sansom. 2001. Simulation approaches to ion channel structure-function relationships. *Q. Rev. Biophys.* 34:473–561.
- Tieleman, D. P., S. J. Marrink, and H. J. C. Berendsen. 1997. A computer perspective of membranes: molecular dynamics studies of lipid bilayer systems. *Biochim. Biophys. Acta*. 1331:235–270.
- Woolf, T., and B. Roux. 1994. Molecular-dynamics simulation of the gramicidin channel in a phospholipid-bilayer. *Proc. Natl. Acad. Sci. U.S.A.* 91:11631–11635.
- Yang, J., A. Y. Ting, P. G. Schultz, and T. Lu. 2000. Gating of a K<sup>+</sup> channel by a dynamic selectivity filter. *Biophys. J.* 78:17a. (Abstr.)
- Zhou, Y., J. H. Morais-Cabral, A. Kaufman, and R. MacKinnon. 2001. Chemistry of ion coordination and hydration revealed by a K<sup>+</sup> channel-Fab complex at 2.0 Å resolution. *Nature*. 414:43–48.